New Results for Coaxial Re-Entrant Cavity with Partially Dielectric Filled Gap

Weiguo Xi, Wayne R. Tinga, *Member, IEEE,* W. A. Geoffrey Voss, and Bai Qiang Tian

Abstract—**Resonant frequencies, Q-factor and electromagnetic field intensity are presented for a set of varied parameters of a coaxial re-entrant cavity with a gap partially filled with a dielectric. The cavity is analyzed using the mode matching technique. The numerical results are found to be in good agreement with experimental data. Based on the numerical results, a scheme for mode identification is proposed and the mode transition is discussed. Furthermore, the equivalent gap capacitances are obtained and compared with the results from an existing formula which has been modified for the dielectric loaded gap.**

I. Introduction

RE-ENTRANT cavities have the advantages of simple mechanical construction and wide tuning range. They have been used effectively in klystrons, solid-state device development and dielectric measurements. Recently, Tinga *et al.* [1] have developed this structure into a microwave applicator for processing and measuring materials with encouraging results. In order to precisely predict its resonant performance, a reliable and efficient theoretical analysis method and design data are required.

Over the past fifty years, many authors have presented the analysis of the re-entrant cavity. Few of them attempted to find a rigorous field solution in a dielectric loaded cavity. Karpova [2] first analyzed a single-post cavity loaded with a dielectric sample having the same diameter as the center conductor. Milewski [3] extended the calculation to the case of a double-post. Recently, Kaczkowski *et al.* [4] developed the formulation further to allow a sample to be smaller than the center conductor. All these analyses were carried out for dielectric measurement purposes. Although some results of frequency shift versus dielectric constant have been presented, the dielectric loading effects on the cavity fields and resonant behavior are not well understood.

The purpose of this paper is to present design data in the form of mode charts and Q-factor diagrams based on numerical results and to interpret these results in order to acquire a better theoretical insight into the resonant characteristics of this structure, enabling us, among others, to design a new high-temperature dielectrometer.

Manuscript received July 10, 1991; revised November 14, 1991. This work was sponsored by the Natural Science and Engineering Research Council of Canada.

The authors are with the Electrical Engineering Department, University of Alberta, Edmonton, AB, Canada T6G 2G7.

IEEE Log Number 9106055.

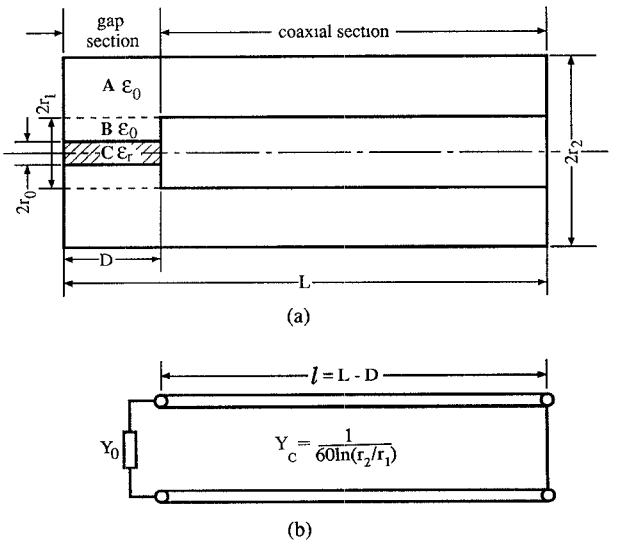

Fig. 1. Single-post coaxial re-entrant cavity with a gap partially filled with a dielectric. (a) Schematic diagram of structure and subareas for mode-matching analysis. (b) Equivalent circuit.

II. Structure and Method

The cavity to be analyzed is a single-post coaxial re-entrant cavity with a partially dielectric filled gap as shown in Fig. 1(a). It has the advantage of easier sample loading [1] than the double-post structure. The method used in the numerical analysis is the mode-matching technique, which was first introduced into cavity analysis by Hahn [5] and was the same method employed by Whinnery *et al.* [6] in their calculations of the step capacitance in coaxial lines.

The structure in Fig. 1(a) can be described as a junction of three subareas, labeled A, B and C. The unknown field in each subarea is expressed in an expansion of respective TM_{on} modes in a circular waveguide as suggested by the structure's axial symmetry. By applying the continuity condition of tangential field components E_z and H_ϕ along the common surface of neighboring subareas, a set of linear equations for individual mode coefficients is obtained. Resonant frequencies and field components can then be solved for. The formulation, which is lengthy but similar to Kaczkowski's [4], is here omitted.

A computer program was implemented for the calculations of resonant frequency, Q-factor and field intensity via the mode-matching formulation. Calculation of the resonant frequency of a given structure, with a truncation error of less than 0.016%, requires a CPU time of about

TABLE I
RESONANT FREQUENCY OF DIELECTRIC LOADED CAVITY
($r_1 = 0.75$, $r_2 = 2.56$, $L = 2.0$, $D = 0.5$ cm)

ϵ_r	f_o (GHz)		Δf(%)
	This Work	Karpova's	
2.495	1.9741	1.9745	−0.02
2.735	1.9184	1.9223	−0.20
3.734	1.7284	1.7322	−0.22
5.605	1.4854	1.4837	0.11
30.83	0.6969	0.6959	0.14

TABLE II
RESONANT FREQUENCY OF EMPTY CAVITY
($r_1 = 1.23$, $r_2 = 4.51$, $L = 20.0$ cm)

D (cm)	f_o (GHz)		Δf(%)
	Calculated	Measured	
0.20	2.3119	2.3131	−0.05
0.50	2.3673	2.3682	−0.04
0.75	2.4047	2.4059	−0.05
1.00	2.4384	2.4380	0.04
1.20	2.4639	2.4649	−0.02
1.50	2.5004	2.5003	0.00
2.00	2.5580	2.5579	0.00
3.00	2.6616	2.6621	−0.02
4.00	2.7375	2.7376	0.00

TABLE III
FREQUENCY SHIFT DUE TO TEFLON SAMPLE
($r_1 = 1.23$, $r_2 = 4.51$, $L = 20.0$, $D = 1.0$ cm)

r_o (cm)	Mode*	Frequency Shift (MHz)		Difference (MHz)
		Calculation	Experiment	
0.75	TEM_4^5	25.9	25.7	0.2
	TEM_4^7	28.0	27.0	1.0
	TEM_4^9	24.3	24.7	−0.4
0.35	TEM_4^5	6.0	6.0	0.0
	TEM_4^7	6.7	7.3	−0.6
	TEM_4^9	5.9	5.4	−0.5

*When the cavity is empty, the measured f_o at TEM_4^5, TEM_4^7 and TEM_4^9 are 1.744, 2.4384, and 3.1341 GHz, respectively.

half a second on our Amdahl 5870 main frame computer. The calculated data were compared with Karpova's and showed a maximum difference of 0.22% as listed in Table I. Table II gives a comparison between the numerical and experimental data for an empty cavity with a varying gap and indicates the discrepancy to be less than 0.05%. Moreover, frequency shifts due to Teflon samples with different radii were measured and are presented in Table III together with the calculation values for three different modes (the mode definition will be given later). The larger errors are believed to be experimental rather than computational. Among the measurement errors, is the frequency measurement error which can be as large as 1 MHz. The error due to possible air gaps at the sample ends should be negligible for low permittivity materials such as Teflon [7].

III. FIELD DISTRIBUTION AND RESONANT MODES

It is known that a standard coaxial cavity has a series of fundamental TEM modes with resonant wavelengths given by

$$\lambda_o = \frac{2}{n} l \tag{1}$$

for a closed cavity and

$$\lambda_o = \frac{4}{2n+1} l \tag{2}$$

for a cavity opened[1] at one end, where $n = 1, 2, \cdots$ and l is the cavity length.

In the presence of a gap in the center conductor as shown in Fig. 1(a), the axial component E_z appears in the gap, hence, the field is no longer an exact TEM field. However, if the gap is much smaller than the wavelength, it is reasonable to expect that the field pattern away from the gap will nearly be TEM except for a change in its resonant wavelength. This is confirmed by the calculated axial field distributions which are depicted in Figs. 2(a) ($\epsilon_r = 1$) and 3(a) ($\epsilon_r = 50$) along with the TEM fields. It is shown that at a distance of $3D$ away from the gap, E_r and H_ϕ are almost the same as those of the TEM fields and E_z, which is associated with TM modes, decays to about 10%. It also shows that the field pattern of $\epsilon_r = 50$ is almost the same as that obtained by stretching the field pattern of $\epsilon_r = 1$ along the z axis, since it is only the resonant wavelength that changes in the coaxial section. However, the net energies stored in the gap section are significantly different. Figs. 2(b) and 3(b) demonstrate the radial distribution of gap fields and clearly show that the gap with $\epsilon_r = 1$ is electrically dominant, i.e., has much more electric energy than magnetic energy, while the gap with $\epsilon_r = 50$ is magnetically dominant. Therefore, it is justified to call the former gap capacitive and the latter inductive. In addition, the gap fields are close to those of the TM_{010} mode in a cylindrical cavity if r is small, i.e., E_z = constant, $H_\phi \alpha J_1(kr)$ and $E_r = 0$. As a result, a rather uniform temperature profile will be achieved when the cavity is used as a microwave applicator.

From the equivalent circuit shown in Fig. 1(b), the resonant condition can be easily written as

$$\cot(l\omega/c) = -jY_o/Y_c \tag{3}$$

where, $Y_o = j\omega C_o$ for a capacitive gap and $Y_o = 1/j\omega L_o$ for an inductive gap. C_o and L_o are the equivalent lumped gap capacitance and inductance and Y_c is the characteristic admittance of the coaxial section. In the case of frequency independent C_o and L_o, the graphical solutions of (3) are reproduced in Fig. 4 to make the following mode definition more explicit.

Fig. 4 shows that the solutions for the resonant frequency of a capacitive gap are all above the horizontal

[1]For this paper, "opened" refers to "ideally opened" which corresponds to a zero fringe capacitance.

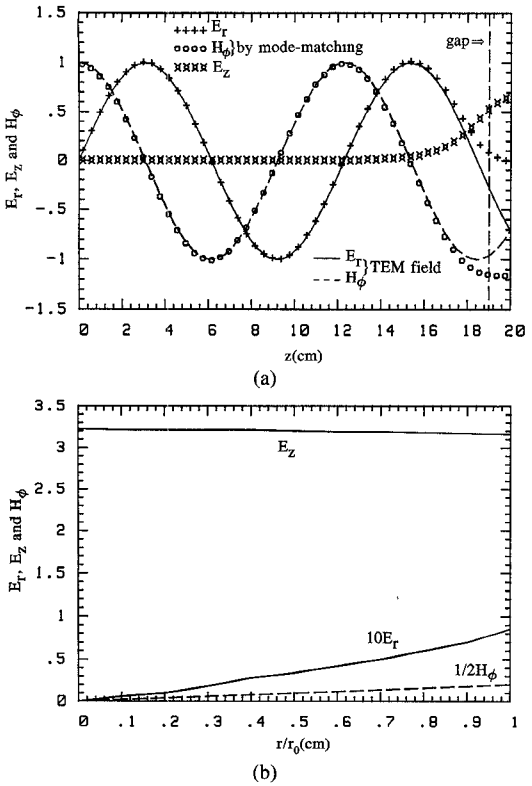

Fig. 2. E and H fields for a capacitive mode ($r_1 = 1.25$, $r_2 = 4.5$, $D = 1.0$, $L = 20.0$, in cm, $\epsilon_r = 1.0$, $f_0 = 2.438$ GHz), normalized by the TEM field in subarea A. (a) Axial distribution in subarea A at $r = 2.875$ cm, compared with the TEM field. (b) Radial distribution in the gap midplane.

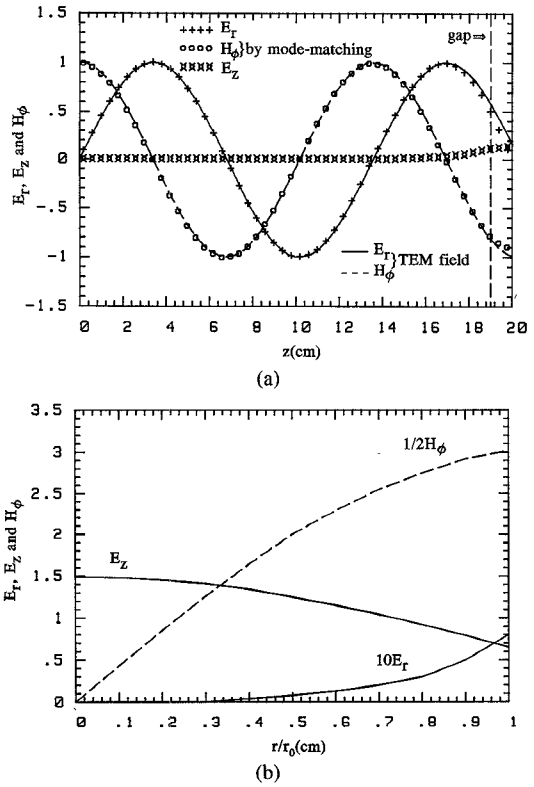

Fig. 3. E and H fields for an inductive mode ($r_1 = 1.25$, $r_2 = 4.5$, $D = 1.0$, $L = 20.0$, in cm, $\epsilon_r = 50.0$, $f_0 = 2.212$ GHz), normalized by the TEM field in subarea A. (a) Axial distribution in subarea A at $r = 2.875$ cm, compared with the TEM field. (b) Radial distribution in the gap midplane.

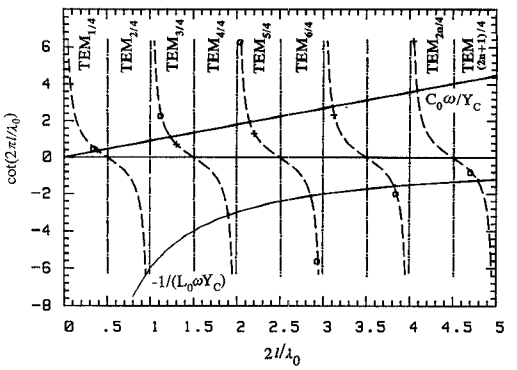

Fig. 4. Graphic solution for resonant frequencies of an ideal coaxial cavity with a constant C_0 or L_0 and the loci of resonant frequencies of a real cavity (+ + +: $\epsilon_r = 10$, ooo: $\epsilon_r = 50$).

axis and between $(n - 1)$ and $(n - 1/2)$, i.e.,

$$(n - 1)\lambda_o/2 < l < (2n - 1)\lambda_o/4 \tag{4}$$

or

$$4l/(2n - 1) < \lambda_o < 2l/(n - 1). \tag{5}$$

These modes are defined as capacitive quasi-TEM modes and designated as $TEM_{(2n-1)/4}$. For an inductive gap, the solutions are all located below the axis and between $(n - 1/2)$ and n, i.e.,

$$(2n - 1)\lambda_o/4 < l < 2n\lambda_o/4 \tag{6}$$

or

$$2l/n < \lambda_o < 4l/(2n - 1). \tag{7}$$

Similarly, these modes are named inductive quasi-TEM modes and designated as $TEM_{2n/4}$. As the gap capacitance disappears or approaches an infinite value, all these quasi TEM modes become exact TEM modes as in an opened or closed coaxial cavity. Compared with a coaxial cavity opened at one end, a capacitive mode (or gap) virtually shortens the cavity whereas an inductive mode (or gap) lengthens the cavity.

Understanding these two types of modes is helpful in making more efficient use of coaxial re-entrant cavities. For example, when designing such a cavity as a microwave power applicator, a capacitive mode should be chosen for heating non-magnetic materials and an inductive mode for magnetic materials so that a maximum material-field interaction and, therefore, a high temperature or heating rate can be obtained.

Generally speaking, the lumped gap parameter C_o or L_o depends not only on cavity dimensions and the sample in the gap but also on resonant modes (or frequency). As shown in Fig. 4, the resonant frequencies of a given cavity, marked by crosses ($\epsilon_r = 10$) and circles ($\epsilon_r = 50$), are no longer located along a straight line or a hyperbolic curve, which means that C_o and L_o are frequency dependent. Nevertheless, it will be shown later that a gap capacitance can be independent of frequency under certain conditions.

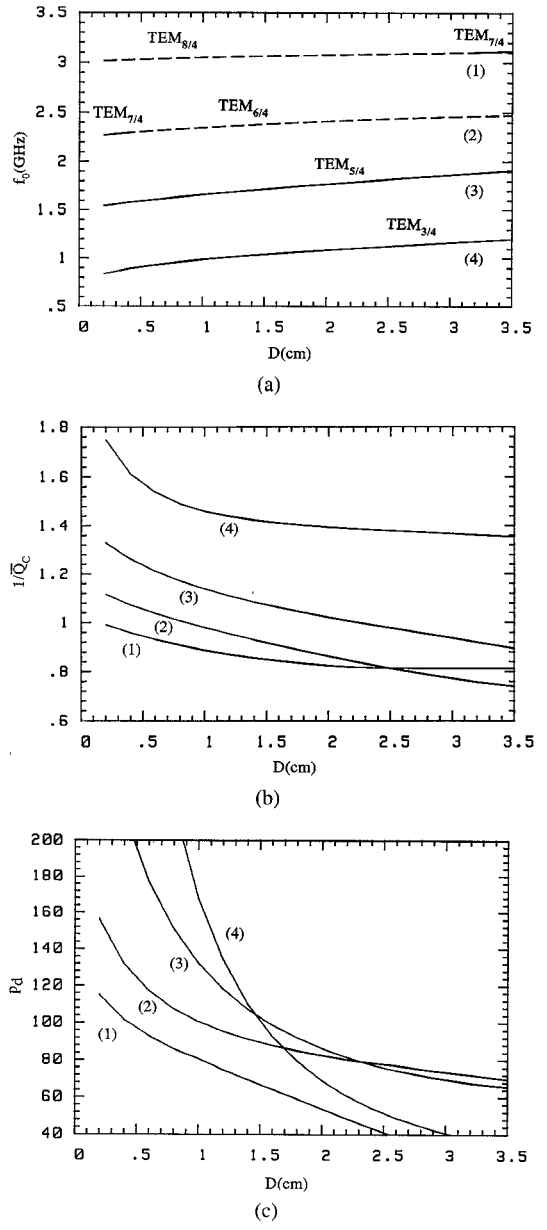

Fig. 5. (a) Resonant frequency. (b) Inverse of normalized cavity Q-factor. (c) Sample energy density, as functions of the gap width, D ($r_0 = 0.5$, $r_1 = 1.25$, $r_2 = 4.5$, $L = 20.0$, in cm, $\epsilon_r = 10$).

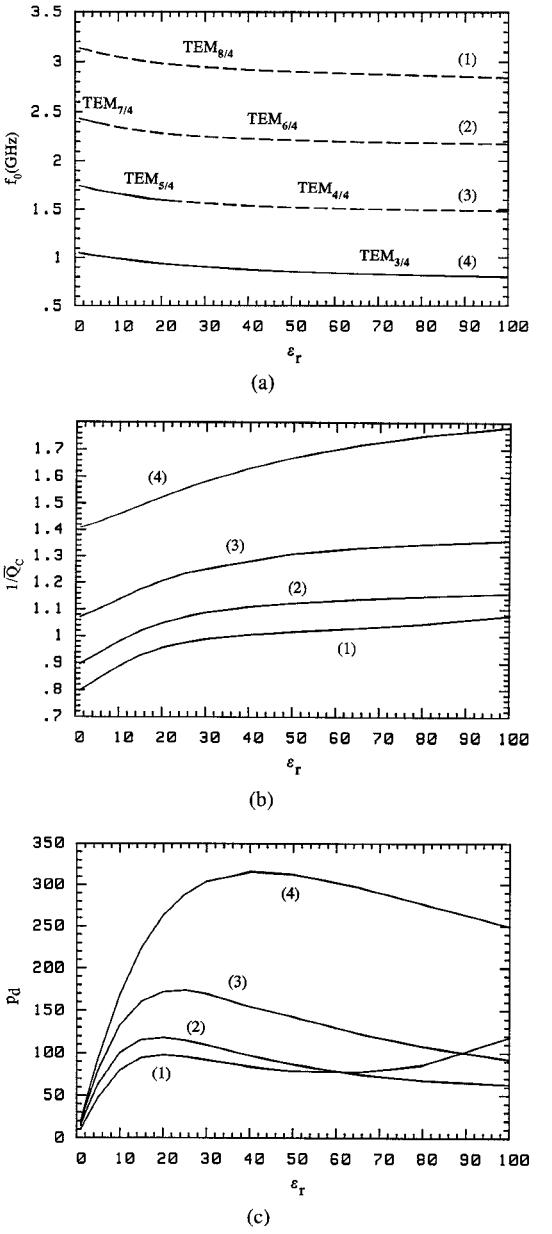

Fig. 6. (a) Resonant frequency. (b) Inverse of normalized cavity Q-factor. (c) Sample energy density, as functions of the dielectric constant, ϵ_r ($r_0 = 0.5$, $r_1 = 1.25$, $r_2 = 4.5$, $L = 20.0$, $D = 1.0$, in cm).

IV. Mode Chart and Q Diagram

Resonant frequency and Q-factor are the two most important parameters of a resonator. These parameters are computed for a typical gap width, D, sample radius, r_o, and sample dielectric constant, ϵ_r, and are presented in Figs. 5–7 in the form of mode charts and normalized Q diagrams.

On the mode charts of Figs. 5(a), 6(a), and 7(a), capacitive modes are shown by solid lines and inductive modes by dashed lines. In contrast to the modes in standard cavities which are distinct from each other, capacitive and inductive modes exhibit a smooth transition between each other as D, r_o and ϵ_r are varied. At the transition point, both the coaxial and gap section have a balance of electric and magnetic energy and are therefore loosely coupled. It is important to understand the mode transition due to the variations in the sample. The mode transition from a capacitive mode to an inductive mode may weaken the interaction of the sample with the electric field. This will cause problems in high temperature material heating since the dielectric constant of most oxides and ceramics increases with temperatures. On the other hand, it is possible to make use of this mode transition to suppress the temperature run-away which arises from the positive temperature coefficient of the material's loss factor. Furthermore, these mode charts show that reducing the gap and increasing the dielectric constant or radius of the sample have an equivalent decreasing effect on resonant frequencies.

The Q-factor of a dielectric loaded cavity is expressed

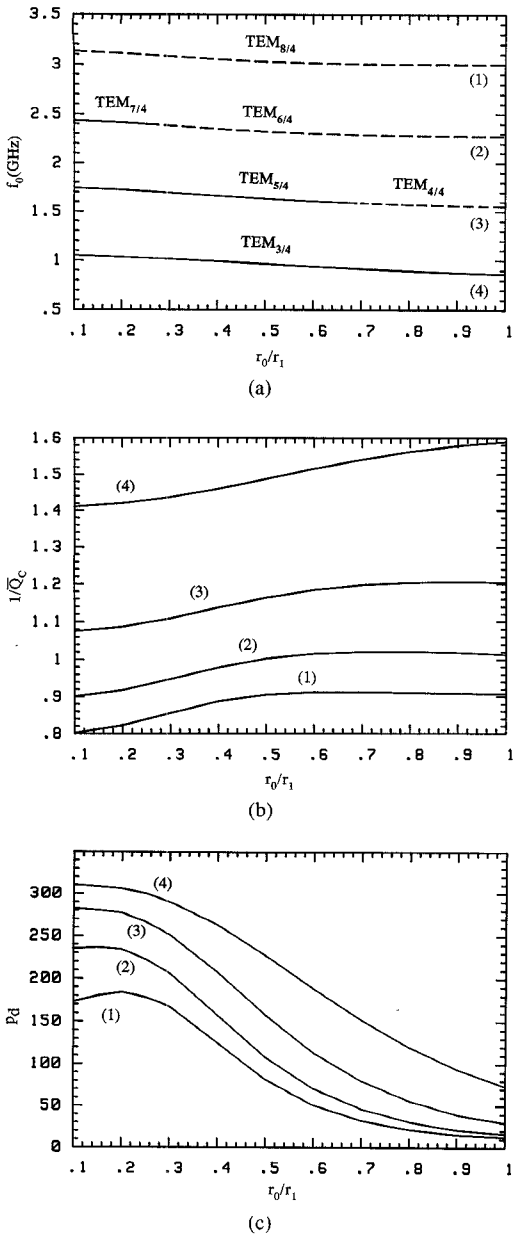

Fig. 7. (a) Resonant frequency. (b) Inverse of normalized cavity Q-factor. (c) Sample energy density, as functions of the normalized sample radius, r_0/r_1 ($r_1 = 1.25$, $r_2 = 4.5$, $L = 20.0$, $D = 1.0$, in cm, $\epsilon_r = 10$).

in two parts as

$$1/Q_o = 1/Q_c + 1/Q_D \tag{8}$$

where, Q_c is cavity Q due to the wall loss and Q_D is cavity Q due to the dielectric loss, i.e.,

$$Q_c = \omega W_E/P_w \tag{9}$$

and

$$Q_D = W_E/(W_D \tan \delta) \tag{10}$$

where, W_E and W_D are the stored energy in the whole cavity and in the sample; P_w is the power dissipated on the cavity walls which is inversely proportional to the square root of the wall conductivity σ. To be useful generally, we define normalized Q-factors $\overline{Q}_c$ and $\overline{Q}_D$, which are independent of σ and $\tan \delta$, as follows

$$\overline{Q}_c = Q_c/\sqrt{\sigma} \tag{11}$$

$$\overline{Q}_D = Q_D \tan \delta = W_E/W_D. \tag{12}$$

The inverse value of a normalized cavity Q-factor, $1/\overline{Q}_c$, is presented as a function of D, ϵ_r and r_o/r_1 in Figs. 5(b), 6(b), and 7(b). Although it seems that the cavity Q-factor varies with D, ϵ_r and r_o in different ways, it is almost always true that Q_c for a set of arbitrary parameters is intrinsically determined by the cavity resonant frequency, that is, Q_c increases with the resonant frequency. An exception may occur if the frequency is so high that the increase in wall loss overrides the increase in the stored energy as shown in Fig. 5(b).

The inverse normalized dielectric Q-factor, $1/\overline{Q}_D$, is equal to the ratio of the energy stored in the sample to that in the cavity. To be more meaningful, $1/\overline{Q}_D$ is divided by a filling factor F and thus becomes an energy density ratio p_d, which determines the heating rate, as follows:

$$p_d = (W_D/V_D)/(W_E/V_C) = 1/(\overline{Q}_D F) \tag{13}$$

$$F = V_D/V_c \tag{14}$$

where, V_D and V_c are the volume of the sample and the cavity. Therefore, Q_D is related to p_d by

$$1/Q_D = \tan \delta/\overline{Q}_D = F p_d \tan \delta. \tag{15}$$

Curves of p_d versus D, ϵ_r and r_o/r_1 are plotted in Fig. 5(c), 6(c), and 7(c). They are clear evidence of a strongly focused electric energy existing in the gap which explains the high heating rate obtained from this structure [1]. However, the focused gap field also imposes limitations on processable volume and loss range of the sample. For example, if $p_d = 500$ and $\tan \delta = 0.1$, a sample with a filling factor of $1/500$ will deteriorate the total cavity Q-factor from any high value, say 2000, to a Q of less than 10. Therefore, it is necessary to reduce the sample volume or increase the input power to maintain a certain heating rate.

In addition, the following conclusions can be drawn from the results of the p_d curves:

(i) The gap energy density rises exponentially as the gap is reduced in Fig. 5(c). An increase in wavelength virtually reduces the gap width which suggests that low frequency operation is preferred to heat samples with practical dimensions.

(ii) In Fig. 6(c), the gap energy density increases almost linearly with ϵ_r for low ϵ_r. It then tends to saturate and drop off slowly with increasing ϵ_r due to the mode shifting away from being a capacitive mode. This relatively flat portion of the curve is advantageous in maintaining a stable heating rate while the sample's dielectric constant varies with temperature.

(iii) The decrease in gap energy density in Fig. 7(c) with increase of sample radius is mainly due to the gap field E_z being approximately a $J_o(kr)$ function which de-

creases with large r. In order to have a relatively uniform field profile, the sample radius should be restricted to less than about 30% of the center conductor radius.

V. Equivalent Gap Capacitance

As mentioned above, a capacitive gap can be represented by a lumped capacitance derived from the known resonant frequency via (3), i.e.,

$$C_o = Y_c \cot (l\omega/c)/\omega \tag{16}$$

On the other hand, Marcuvitz [8] gave an expression for the equivalent capacitance of an empty gap as follows:

$$C_o^* = \epsilon_o \pi r_1^2/D + 4\epsilon_o r_1 ln((r_2 - r_1)/D). \tag{17}$$

This capacitance is composed of a parallel plate capacitance

$$C_{op}^* = \epsilon_o \pi r_1^2/D \tag{18}$$

and a fringe capacitance

$$C_{of}^* = 4\epsilon_o r_1 ln((r_2 - r_1)/D). \tag{19}$$

To extend the expression to the case of a partially dielectric filled gap, C_{op}^* can be modified as

$$C_{op}^* = \pi\epsilon_o(r_o^2(\epsilon_r - 1) + r_1^2)/D \tag{20}$$

and C_{of}^* remains unchanged. Therefore, (17) becomes

$$C_o^* = \pi\epsilon_o(r_o^2(\epsilon_r - 1) + r_1^2)/D + 4\epsilon_o r_1 ln((r_2 - r_1)/D). \tag{21}$$

To examine the validity of (21), a comparison between C_o^* of (21) and C_o of (16) is made and presented in Fig. 8 for different radii and dielectric constant of the sample. These curves show that (21) is valid if the gap width is much smaller than the wavelength in the dielectric. We can adopt the same conditions as given by Marcuvitz, that is, $2\pi D/\lambda << 1$ and $D/(r_2 - r_1) << 1$, where $\lambda = \lambda_o/\sqrt{\epsilon_r}$ is the wavelength in the dielectric.

VI. Conclusion

The results and analysis presented in this paper show that the re-entrant gap loaded with a dielectric sample has a pronounced effect on the resonant frequency and energy storage, especially in the case of a high dielectric constant or a large sample volume or a narrow gap. As a result, a high sensitivity for dielectric determinations and a high heating rate for material processing can be achieved when this structure is used as a dielectrometer and a microwave applicator. The proposed mode designation, though simple, gives qualitative insight into the cavity field, which in turn helps in the design of practical resonant applicators. The mode-charts and Q diagrams provide further quantitative information for the design of efficient resonators. Finally, a modified design formula for the equivalent gap capacitance is shown to be an acceptable approximation for a narrow gap.

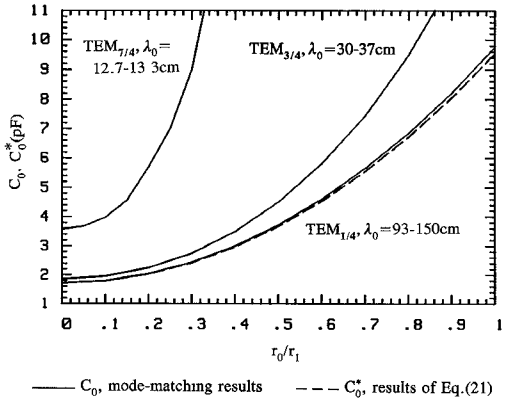

(a)

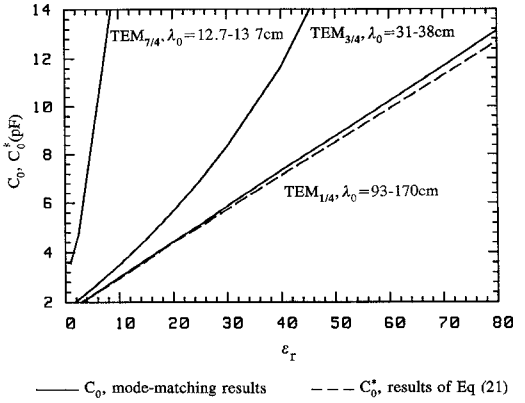

(b)

Fig. 8. Equivalent gap capacitance ($r_1 = 1.25$, $r_2 = 4.5$, $L = 20.0$, $D = 0.5$, in cm) versus (a) sample radius ($\epsilon_r = 10$) and (b) dielectric constant ($r_0 = 0.5$ cm).

References

[1] W. R. Tinga, B. Q. Tian, and W. A. G. Voss, "New high temperature multipurpose applicator," *Mat. Res. Soc. Proc.*, vol. 189, pp. 111–116, 1991.

[2] O. V. Karpova, "On an absolute method of measurement of dielectric properties of a solid using a π-shaped resonator," (in Russian), *Fiz. Twerd. Tela*, vol. 1, pp. 246–255, Feb. 1959, Moscow.

[3] A. Milewski, "Coaxial lumped capacitance resonators for the investigations of dielectrics," *Electron Techn.*, vol. 10, pp. 71–98, Jan. 1977, Warszawa.

[4] A. Kaczkowski and A. Milewski, "High-accuracy wide-range measurement method for determination of complex permittivity in re-entrant cavity: Part A—Theoretical analysis of the method," *IEEE Trans. Microwave Theory Tech.*, vol. MTT-28, pp. 225–228, Mar. 1980.

[5] W. C. Hahn, "A new method for the calculation of cavity resonators," *J. Appl. Phys.*, vol. 12, pp. 63–68, Jan. 1941.

[6] J. R. Whinnery, H. W. Jamieson, and T. E. Robbins, "Coaxial-line discontinuity," *Proc. IRE*, pp. 695–709, Nov. 1944.

[7] A. Kaczkowski and A. Milewski, "High-accuracy wide-range measurement method for determination of complex permittivity in re-entrant cavity—Part B—experimental analysis of measuring erros," *IEEE Trans. Microwave Theory Tech.*, vol. MTT-28, pp. 228–231, Mar. 1980.

[8] N. Marcuvitz, *Waveguide Handbook*. New York: McGraw-Hill, 1951, p. 178.

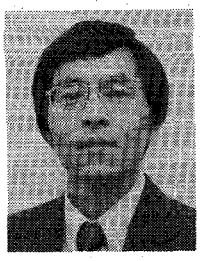

Weiguo Xi was born in China in 1959. He received the B.Sc. and the M.Sc. degrees in electronic engineering from Southeast University (formerly Nanjing Institute of Technology) in 1982 and 1985, respectively.

He then joined the Electronics Research Institute of Southeast University, working as a Researcher and Lecturer in the theory of electron optics and the design of electron guns until 1989. Since then, he has been working towards the Ph.D. degree in electrical engineering at the University of Alberta, Edmonton, AB, Canada. His current research interests include dielectric measurements, microwave heating and numerical analysis of microwave resonators.

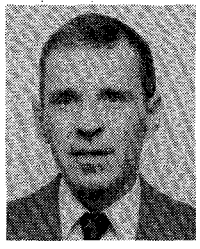

Wayne R. Tinga (S'62–M'68) was born in the Netherlands in 1938 and immigrated to Canada in 1953. He received the Ph.D. degree in electrical engineering in 1969 from the University of Alberta, Edmonton, AB, Canada.

He became Assistant Professor in 1970, Associate Professor in 1974 and Full Professor in 1980 at the University of Alberta. He was on leave with Litton Microwave Cooking R/D Labs from 1979–1980 where he worked on developing one of his patents on frequency agile computer controlled microwave ovens. He was made a Fellow in the International Microwave Power Institute (IMPI) in 1980 after having served IMPI in many capacitances since its inception in 1966. He held the IMPI offices of President, Board Chairman, Executive Director, Symposium Chairman, and Technical Program Co-Chairman. He also served on many technical committees dealing with frequency allocations, radio frequency interference and safety standards. He served as Associate Editor of the Journal of Microwave Power (1970–1978), its Editorial Review Board (1978–present), and is on the review board of IEEE TRANSACTIONS ON GEOSCIENCE AND REMOTE SENSING (1988–1991). From 1983–1986, he was on leave to Dordt College, Sioux Center, IA, where he put in place a four-year electrical engineering program. After his return to the University of Alberta, he was acting Director of Computer Engineering (1987–1988). For over 25 years, he has engaged in the industrial, scientific, medical and domestic applications of microwave energy. His active research dealt with microwave dielectric properties, measurement techniques, microwave power system design and dielectric mixture modelling. He developed new dielectric measurement techniques and an advanced dielectric mixture theory to predict behavior of the microwave properties of materials. He has been an active consultant to major corporations in the automotive,food, plastic, nuclear, aluminum, microwave oven, forest products and space industries. He has published over 60 technical papers and co-authored a number of tutorial books on microwave power. Currently, he is pursuing research in the area of high temperature dielectric measurement methods and modeling.

Dr. Tinga is a member of the Professional Engineering Association of Alberta, IMPI, the American Ceramics Society and the Materials Research Society.

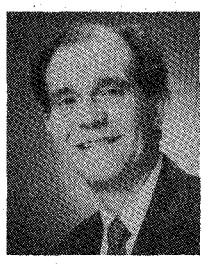

W. A. Geoffrey Voss received the B.Sc. degree in electrical engineering from Queen Mary College, University of London, UK in 1957 and the Ph.D. degree from the University of London, in 1961. He was awarded a BBC Research Scholarship in 1960 and went to the University of BC, Canada on a NATO Graduate Exchange Scholarship in 1961.

In 1964 he joined the University of Alberta where he worked, off and on, for 25 years. He has been Editor of the *Journal of Microwave Power and Electromagnetic Energy* for some 14 years of its 26 year history and was one of the founders of the International Microwave Power Institute in 1966. He is now Professor Emeritus, Engineering and Medicine, at the University of Alberta and President, Voss Associates Engineering Ltd., a Victoria, BC consulting company, which he started in 1981.

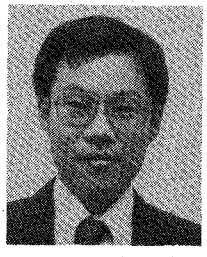

Bai Qiang Tian was born in Shichuan, China, in October 1959. He received the B.Sc. and M.Sc. degrees from the University of Electronic Science and Technology of China, Chengdu, China, in 1981 and 1987, respectively.

He was a Lecturer in the Department of Electromagnetic Field Engineering at the University of Electronic Science and Technology of China from 1981 to 1987. He is currently working towards the Ph.D. degree in electrical engineering at the University of Alberta, Edmonton, AB, Canada. His research interests include microwave measurement, microwave material processing and applicator design.